Inorganica Chimica Acta 440 (2016) 107–117

Contents lists available at ScienceDirect

Inorganica Chimica Acta

journal homepage: www.elsevier.com/locate/ica

Synthesis and crystal structures of a series of (μ-thiophenolato)(μ-pyrazolato-*N*,*N*′) double bridged dipalladium(II) complexes and their application in Mizoroki–Heck reaction as highly efficient catalysts

Narjes Khadir [a,*], Ghazal Tavakoli [a], Abdeljalil Assoud [b], Mojtaba Bagherzadeh [a], Davar M. Boghaei [a,*]

[a] Chemistry Department, Sharif University of Technology, P.O. Box 11155-3615, Tehran, Iran
[b] Department of Chemistry, University of Waterloo, Waterloo, Ontario N2L 3G1, Canada

ARTICLE INFO

Article history:
Received 31 July 2015
Received in revised form 15 September 2015
Accepted 16 October 2015
Available online 3 November 2015

Keywords:
Binucleating S-protected ligand precursors
Binuclear Pd(II) complexes
Single crystal X-ray diffraction study
Mizoroki–Heck reaction
Catalytic activity

ABSTRACT

Three new binucleating S-protected ligand precursors, 2-(*N*,*N*-dimethylthiocarbamato)-5-methylisophthalaldehyde di-2′-hydroxy 5′-methylanil (**1b**), 2-(*N*,*N*-dimethylthiocarbamato)-5-*tert*-butylisophthalaldehyde di-2′-hydroxyanil (**2a**) and 2-(*N*,*N*-dimethylthiocarbamato)-5-*tert*-butylisophthalaldehyde di-2′-hydroxy 5′-methylanil (**2b**), have been synthesized. The reaction of these ligand precursors with $PdCl_2$ in the presence of pyrazole under Pd-mediated S–C cleavage yielded a series of binuclear palladium(II) complexes of general formula [LPd_2(pz)], where pz is the exogenous bridging pyrazolyl ligand and L^{3-} represents a series of pentadentate thiophenol-based bridging ligands originated from their corresponding ligand precursors. All the compounds were characterized by elemental analysis, IR, ^{1}H NMR and UV–Vis spectroscopies. The binuclear μ-thiophenolato-μ-pyrazolato palladium(II) complexes have also been characterized by single crystal X-ray diffraction analysis. Crystal structure analyses of the complexes show that two Pd^{II} centers are located in distorted square-planar environments, arranged in binuclear units with Pd···Pd distance of 3.57 Å. The catalytic activity of these new binuclear palladium complexes was studied in Mizoroki–Heck C–C coupling reaction of methyl- and *n*-butyl acrylate with various types of aryl iodides and bromides. All reactions were completed for very short times with very excellent yield. Reactions were stereoselective and only *trans* isomers were obtained in each case.

1. Introduction

The Heck reaction, palladium-catalyzed carbon–carbon bond formation between aryl halides and olefins, has become one of the most fundamental reactions for the synthesis of various bioactive compounds, natural products and industrially important organic frameworks over the past few decades [1–4]. To date, many efforts have been made to develop more efficient and selective catalytic systems for this kind of reactions using various palladium catalysts [5–8]. In this context, design and synthesis of new ligands and their palladium(II) complexes that can act as a potential catalysts for the Heck reaction with enhanced reactivity toward less activated aryl bromides and chlorides has received considerable attention and is the current hot topic of research [4]. Toward this point, mononuclear palladium(II) complexes have been the most extensively studied catalytic systems for Heck reaction [9–13]. However, reports on catalytic application of binuclear palladium(II) complexes based on binucleating ligands are still rare in this reaction and essentially limited to only a few complexes with ligands that cause large metal–metal separations [14,15].

Indeed, binuclear palladium(II) complexes supported by binucleating compartmental ligands, i.e. "ligands comprising two adjacent coordination sites in which the central donor atom(s) provide a bridge", are interesting in view of the expectation that two metal centers in close proximity could exhibit inter-metallic cooperative effect and thus their reactivity in synthesis and catalysis may differ significantly from that of analogous mononuclear complexes [16–24].

Among the various types of binucleating compartmental ligands causing relatively short metal–metal distances (3.0–4.0 Å) [25], thiophenol-based compartmental ligands have established themselves as a privileged class of ligands in preparation of binuclear palladium(II) complexes [26–29]. Despite the fact that thiophenolates produce an especially rich class of sulfur–metal complexes [30], binucleating compartmental thiophenolate ligands are often less studied than their corresponding phenolates

* Corresponding authors. Tel.: +98 21 6600571; fax: +98 21 66012983.
E-mail addresses: narjes.khadir@yahoo.com (N. Khadir), dboghaei@sharif.ir (D.M. Boghaei).

http://dx.doi.org/10.1016/j.ica.2015.10.035
0020-1693/

[31]. This is mainly because of their facile redox activity and the difficulties associated with their synthetic procedure [30,32–34]. These synthetic problems can be overcome to some extent by introducing the sulfur function as a sulfur protected-group [35]. To date, thioethers [32,36] and thiocarbamates [26,37,38] thanks to their relative lack of chemical reactivity, have proven to be useful protective groups for thiophenolates.

During our efforts to synthesize and study such systems, we have prepared and characterized a number of compartmental S-protected ligand precursors belonging to the class introduced by Robson et al. [39,40], that is, pentadentate Schiff-base ligands derived from the condensation of 2 equiv. of *o*-aminophenol or 2-amino-4-methylphenol with 1 equiv. of the 2-(*N,N*-dimethylthiocarbamato)-isophthalaldehyde of 5-^{t}Bu or 5-Me (Scheme 1). These ligand precursors would then serve as an *in situ* source of L^{3-} in the synthesis of complexes by a metal-ion-promoted S-deprotection process [39–41]. Herein, we report the synthesis, spectroscopic characterization and crystal structures of four new binuclear palladium(II) complexes of general formula [LPd_2(pz)] {pz = the exogenous bridging pyrazolyl ligand; L = 2,6-bis[(2-phenoxy) iminomethyl]-4-methylthiophenolate (L^{1a}), 2,6-bis{[(2-hydroxy-5methylphenyl)imino]methyl}-4-methylthiophenolate (L^{1b}), 2, 6-bis[(2-phenoxy)iminomethyl]-4-*tert*-butylthiophenolate (L^{2a}) or 2,6-bis{[(2-hydroxy-5methylphenyl)imino]methyl}-4-*tert*-butylthiophenolate (L^{2b})}. These new complexes were evaluated as catalysts for the Heck C–C coupling reactions. To the best of our knowledge, this study presents the first catalytic employment of bridged binuclear palladium(II) complexes with relatively short metal–metal distances (3.57 Å) in Mizoroki–Heck C–C coupling reaction. In these reactions, methyl- and *n*-butyl acrylate was reacted with various types of aryl halides including aryl iodides and bromides. All reactions were completed during short reaction times in the range of 30–140 min with very excellent conversions and stereospecificity for the production of only *trans* isomer.

2. Experimental

2.1. Materials

2-(*N,N*-dimethylthiocarbamato-S)-5-methylisophthalaldehyde [42], 2-(*N,N*-dimethylthiocarbamato-S)-5-*tert*-butylisophthalaldehyde [43], and 2-(*N,N*-dimethylthiocarbamato)-5-methylisophthalaldehyde di-2′-hydroxyanil, ***1a*** [40], were prepared from the literature methods. All other materials were used as supplied by commercial sources.

2.2. Physical measurements

Elemental analyses were performed on a Fison equipment, model EA 1108. UV–Vis spectra were recorded with a CARY 100 Bio VARIAN UV–Vis spectrophotometer using quartz cells having a 1.0 cm path length. Infrared spectra (4000–400 cm^{-1}) of solid samples were taken as a 1% dispersion in KBr pellets using a Unicam Matson 1000 FT-IR spectrophotometer. ^{1}H NMR spectra were recorded on a Bruker 500-DRX Avance spectrometer. Chemical shifts for NMR spectra are referenced to TMS. Melting points of the products were monitored on a BUCHI Melting Point Model B-540 apparatus and are uncorrected. Gas chromatography (GC) analyses were performed on an Agilent Technologies 6890N, equipped with a 19019J-413 HP-5, 5% phenyl methyl siloxane, capillary column (60.0 m × 250μm × 1.00 μm).

2.3. Crystal structure determination

The crystal structures of complexes **1**–**4** were established using X-ray diffraction. Crystallographic data and structural refinements are given in Table 1. Selected bond lengths and bond angles are listed in Table 2. Diffraction data were collected on a Bruker Kappa APEX II diffractometer using graphite-monochromated Mo Kα radiation (λ = 0.71073 Å). Data were collected using ω- and ϕ- scans of 0.3° in groups of frames at different ω and ϕ with exposure times of 10–30 s per frame depending on the crystal scattering. They were corrected for Lorentz and polarization effects using the Bruker SAINT software package [44]. Absorption corrections were based on fitting a function to the empirical transmission surface as sampled by multiple equivalent measurements using SADABS [45].

All structures were solved using the direct method and refined using the least squares method with the Bruker SHELXTL software package [46]. All hydrogen atoms in geometrically idealized positions were refined using a rigid model with C–H = 0.93–1 Å and isotropic displacement parameters Uiso(H) = 1.2 Ueq(C) – 1.5 Ueq(C).

2.4. Synthesis of precursor compounds

2.4.1. 2-(N,N-dimethylthiocarbamato)-5-methylisophthalaldehyde di-2′-hydroxy 5′-methylanil (*1b*)

To a solution of 2-amino-4-methylphenol (1.08 g, 8.8 mmol) in methanol (10 mL) was added 2-(*N,N*-dimethylthiocarbamato-S)-5-methylisophthalaldehyde (1 g, 4 mmol) in boiling methanol

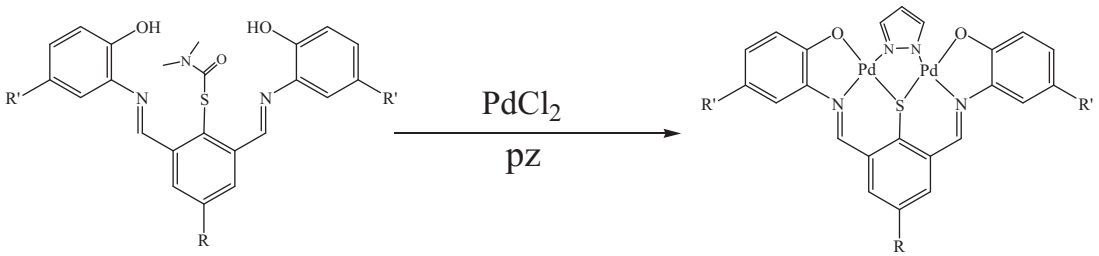

R	R'	Ligand precursor	Complex
H	Me	1a	1
Me	Me	1b	2
H	*tert*-butyl	2a	3
Me	*tert*-butyl	2b	4

Scheme 1. Synthesis of binuclear palladium(II) complexes [LPd_2(pz)].

Table 1
Crystal data and structure refinement for complexes [$L^{1a}Pd_2(pz)$] (**1**), [$L^{1b}Pd_2(pz)$] (**2**), [$L^{2a}Pd_2(pz)$] (**3**) and [$L^{2b}Pd_2(pz)$] (**4**).

Empirical formula	$C_{24}H_{18}N_4O_2Pd_2S$ (**1**)	$C_{26}H_{22}N_4O_2Pd_2S$ (**2**)	$C_{27}H_{24}N_4O_2Pd_2S$ (**3**)	$C_{29}H_{23}N_4O_2Pd_2S$ (**4**)
Formula weight	639.28	667.33	681.36	704.37
T (K)	296(2)	296(2)	293(2)	296(2)
λ (Å)	0.71073	0.71073	0.71073	0.71073
Crystal system	monoclinic	monoclinic	tetragonal	monoclinic
Space group	$P2_1/c$	$P2_1/n$	$P\text{-}42_1c$	$P2_1/c$
Crystal color, shape	Red, needle	Red, needle	Red, needle	Red, needle
Crystal size, mm × mm × mm	0.02 × 0.04 × 0.28	0.01 × 0.02 × 0.32	0.01 × 0.02 × 0.44	0.01 × 0.04 × 0.32
a (Å)	9.1912(10)	8.0866(12)	26.8892(3)	7.088(3)
b (Å)	19.1698(3)	22.217(4)	26.8892(3)	27.591(9)
c (Å)	12.4880(2)	13.322(2)	7.02430(10)	27.793(9)
α (°)	90	90	90	90
β (°)	106.0640(8)	100.956(10)	90	95.498(20)
γ (°)	90	90	90	90
V (Å^3)	2114.39(5)	2349.7(7)	5078.77(13)	5411(3)
μ (mm^{-1})	1.832	1.653	1.531	1.441
D_{calc} (g/mL)	2.0083(1)	1.8864(6)	1.7823(1)	1.729
Z	4	4	8	8
$F(000)$	1256	1320	2704	2792
θ range for data collection (°)	2.125–28	1.807–26	1.1–28	0.738–28.000
Index ranges	$-12 \leqslant h \leqslant 12$ $-25 \leqslant k \leqslant 25$ $-16 \leqslant l \leqslant 16$	$-8 \leqslant h \leqslant 9$ $-27 \leqslant k \leqslant 27$ $-16 \leqslant l \leqslant 16$	$-35 \leqslant h \leqslant 34$ $-35 \leqslant k \leqslant 34$ $-9 \leqslant l \leqslant 9$	$-18 \leqslant h \leqslant 18$ $-20 \leqslant k \leqslant 20$ $-16 \leqslant l \leqslant 16$
Maximum and minimum transmission	0.7460 and 0.7087	0.745987 and 0.309253	0.7460 and 0.6926	0.7459 and 0.3738
Refinement method	Full-matrix least-squares on F^2	Full-matrix least-squares on F^2	Full-matrix least-squares on F^2	Full-matrix least-squares on F^2
Goodness-of-fit on F^2	1.015	0.979	0.979	0.906
R_1 and wR_2 indices [$I > 2\sigma(I)$]	$R_1 = 0.0308$, $wR_2 = 0.0526$	$R_1 = 0.0843$, $wR_2 = 0.1677$	$R_1 = 0.0302$, $wR_2 = 0.0712$	$R_1 = 0.1474$, $wR_2 = 0.2233$
R_1 and wR_2 indices (all data)	$R_1 = 0.0543$, $wR_2 = 0.0596$	$R_1 = 0.2003$, $wR_2 = 0.1966$	$R_1 = 0.0427$, $wR_2 = 0.0904$	$R_1 = 0.4159$, $wR_2 = 0.3374$
Largest difference in peak and hole (e Å^{-3})	0.464 and −0.368	1.575 and −1.384	0.563 and −0.457	1.396 and −1.620

(20 mL). The resulting red solution was heated under reflux for 10 min; then, allowed to cool down to room temperature. The product separated as yellow precipitate of the dimethylcarbamoyl-sulphur-protected ligand, was collected by filtration, washed with methanol and was air dried. M.P. = 203–206 °C, yield: 93.27%. *Anal.* Calc. for $C_{26}H_{27}N_3O_3S$: C, 67.66; H, 5.90; N, 9.10; S, 6.95. Found: C, 67.53; H, 5.80; N, 9.13; S, 6.90%. IR (KBr, cm^{-1}): 3408 ν(OH), 3026 ν(C–H_{ar}), 2920 and 2862 ν(C–H_{al}) 1664 ν(C=O), 1616 ν(C=N), 1488 ν(C=C). UV–Vis (MeOH), [λ_{max}, nm (ε, L mol^{-1} cm^{-1})]: 363 (1664), 266 (3455), 204 (7476). ^{1}H NMR (δ ppm in $CDCl_3$): 9.22 (s, 2H, imine), 8.19 (s, 2H, protons of central aromatic ring), 6.96–7.1 (m, 8H, 2-imino-4-methylphenolic and $OH_{phenolic}$ protons), 3.26 and 3.04(b, 6H, $N(CH_3)_2$), 2.5 (s, 3H, CH_3), 2.33 (s, 6H, CH_3).

2.4.2. 2-(N,N-dimethylthiocarbamato)-5-tert-butylisophthalaldehyde di-2′-hydroxyanil (**2a**)

The 2-(*N,N*-dimethylthiocarbamato)-5-*tert*-butylisophthalaldehyde di-2′-hydroxyanil compound, **2a**, was prepared from the previously described procedure for **1b**, using 2-(*N,N*-dimethylthiocarbamato-S)-5-*tert*-butylisophthalaldehyde and *o*-Aminophenol instead of 2-(*N,N*-dimethylthiocarbamato-S)-5-methylisophthalaldehyde and 2-amino-4-methylphenol respectively. M.P. = 203–206 °C, yield: 93.16%. *Anal.* Calc. for $C_{27}H_{29}N_3O_3S$: C, 68.19; H, 6.15; N, 8.84; S, 6.74. Found: C, 68.03; H, 6.2; N, 8.75; S, 6.76%. IR (KBr, cm^{-1}): 3367 ν(OH), 3047 ν(C–H_{ar}), 2964 ν(C–H_{al}), 1664 ν(C=O), 1617 ν(C=N), 1504 ν(C=C). UV–Vis (MeOH), [λ_{max}, nm (ε, L mol^{-1} cm^{-1})]: 356 (2172), 273 (3606), 253 (3805), 206 (10422). ^{1}H NMR (δ ppm in $CDCl_3$): 9.27 (s, 2H, imine), 8.44 (s, 2H, protons of central aromatic ring), 7.284–7.187 (m, 6H, *o*-iminophenolic and $OH_{phenolic}$ protons), 7.041 (d, J = 7.5 Hz, 2H, *o*-iminophenolic protons), 6.93 (t, J = 7 Hz, 2H, *o*-iminophenolic protons), 3.23 and 3.02(b, 6H, $N(CH_3)_2$), 1.44 (s, 9H, *tert*-butyl).

2.4.3. 2-(N,N-dimethylthiocarbamato)-5-tert-butylisophthalaldehyde di-2′-hydroxy 5′-methylanil (**2b**)

The 2-(*N,N*-dimethylthiocarbamato)-5-*tert*-butylisophthalaldehyde di-2′-hydroxy 5′-methylanil compound, **2b**, was prepared from the previously described procedure for **1b**, using 2-(*N,N*-dimethylthiocarbamato-S)-5-*tert*-butylisophthalaldehyde instead of 2-(*N,N*-dimethylthiocarbamato-S)-5-methylisophthalaldehyde. M.P. = 203–206 °C, yield: 93.56%. *Anal.* Calc. for $C_{29}H_{34}N_3O_3S$: C, 69.02; H, 6.79; N, 8.33; S, 6.35. Found: C, 69.13; H, 6.63; N, 8.49; S, 6.42%. IR (KBr, cm^{-1}): 3421 ν(OH), 3018 ν(C–H_{ar}), 2960 and 2923 ν(C–H_{al}), 1668 ν(C=O), 1620 ν(C=N), 1500 ν(C=C). UV–Vis (MeOH), [λ_{max}, nm (ε, L mol^{-1} cm^{-1})]: 364 (2544), 287 (2988), 246 (4036), 205 (9582).^{1}H NMR (δ ppm in $CDCl_3$): 9.24 (s, 2H, imine), 8.42 (s, 2H, protons of central aromatic ring), 7.07–6.91 (m, 8H, 2-imino-4-methylphenolic and $OH_{phenolic}$ protons), 3.25 and 3.03 (b, 6H, $N(CH_3)_2$), 2.34 (s, 6H, CH_3), 1.54 (s, 9H, *tert*-butyl).

Table 2
Selected interatomic bond distances (Å) and angles (°) for complexes [$L^{1a}Pd_2(pz)$] (**1**), [$L^{1b}Pd_2(pz)$] (**2**), [$L^{2a}Pd_2(pz)$] (**3**) and [$L^{2b}Pd_2(pz)$] (**4**).

Compound	[$L^{1a}Pd_2(pz)$] (**1**)	[$L^{1b}Pd_2(pz)$] (**2**)	[$L^{2a}Pd_2(pz)$] (**3**)	[$L^{2b}Pd_2(pz)$] (**4**)
Pd1–O1	2.006(2)	2.038(10)	2.015(5)	2.047(17)
Pd1–N3	2.006(2)	2.018(13)	2.012(5)	2.017(14)
Pd1–S1	2.1981(9)	2.206(4)	2.2180(17)	2.227(6)
Pd1–N1	1.993(2)	1.976(13)	1.985(5)	2.003(14)
Pd2–O2	2.017(3)	2.023(11)	2.024(4)	2.046(15)
Pd2–N4	2.005(3)	1.991(12)	2.004(5)	2.027(17)
Pd2–S1	2.2017(9)	2.200(4)	2.2148(17)	2.217(5)
Pd2–N2	1.992(3)	1.977(13)	1.985(5)	1.979(16)
O1–Pd1–S1	171.48(8)	172.9(3)	174.71(16)	171.9(4)
N1–Pd1–N3	176.94(10)	178.0(5)	176.8(2)	177.2(7)
Pd1–S1–Pd2	109.0(3)	108.16(16)	107.35(7)	107.2(2)
C1–S1–Pd1	111.76(10)	110.2(4)	109.5(2)	112.1(7)
N4–Pd2–N2	178.29(11)	177.2(5)	176.7(2)	177.6(6)
S1–Pd2–O2	173.58(7)	171.7(3)	173.67(16)	173.6(4)
C1–S1–Pd2	111.49(10)	110.8(5)	110.2(2)	111.3(6)

2.5. Synthesis of binuclear palladium(II) complexes

2.5.1. [$L^{1a}Pd_2(pz)$] (**1**)

A solution containing 0.014 g of the S-protected ligand precursor **1a** (0.032 mmol) and 0.02 g of pyrazole (0.032 mmol) in 5 mL

of boiling acetonitrile (CH_3CN) was added to a hot solution of 0.012 g of palladium(II) chloride (0.064 mmol) in 3 mL of DMSO. The intense red solution was filtered and then remained at room temperature for two days. Crystals of [$L^{1a}Pd_2(pz)$] (**1**) were collected by filtration, washed with acetonitrile and dried at 80 °C under vacuum. Yield: 0.012 g (60%). *Anal.* Calc. for $C_{24}H_{18}N_4O_2Pd_2S$: C, 45.09; H, 2.84; N, 8.76; S, 5.02. Found: C, 44.08; H, 2.76; N, 8.59; S, 5.20%. IR (KBr, cm^{-1}): 3029 ν(C–H_{ar}), 2921 ν(C–H_{al}), 1666–1590 br ν(C=N_{pz}) and ν(C=N (L^{1a})), 1463 ν(C=C), 540 ν(Pd–N). UV–Vis (DMF), [λ_{max}, nm (ε, L mol^{-1} cm^{-1})]: 518 (1258), 365 (1957), 308 (2193), 234 (3257). ^{1}H NMR (δ ppm in DMSO-d_6): 8.99 (s, 2H, imine), 8.11 (s, 2H, protons of central aromatic ring), 7.84 (d, J = 7.5 Hz, 2H, *o*-iminophenolic protons) 7.59 (d, J = 0.7 Hz, 2H, pyrazolic protons), 7.16 (t, J = 7.0 Hz, 2H, *o*-iminophenolic protons), 6.84 (d, J = 8.5 Hz, 2H, *o*-iminophenolic protons), 6.57 (t, J = 7.5 Hz, 2H, *o*-iminophenolic protons), 6.22 (bs, 1H, pyrazolic protons), solvent peak obscures the signal arising from protons of methyl group attached to central aromatic ring.

2.5.2. [$L^{1b}Pd_2(pz)$] (**2**)

The complex [$L^{1b}Pd_2(pz)$] was prepared in a similar method to that of complex [$L^{1a}Pd_2(pz)$] (**1**) except that **1b** was used in the preparation instead of **1a**. Yield: 70%. *Anal.* Calc. for $C_{26}H_{22}N_4O_2Pd_2S$: C, 46.79; H, 3.32; N, 8.40; S, 4.80. Found: C, 46.69; H, 3.36; N, 8.47; S, 4.72%. IR (KBr, cm^{-1}): 3056 ν(C–H_{ar}), 2920 ν(C–H_{al}), 1663–1610 br ν(C=N_{pz}) and ν(C=N (L^{1b})), 1477 ν(C=C), 542 ν(Pd–N). UV–Vis (DMF), [λ_{max}, nm (ε, L mol^{-1} cm^{-1})]: 514 (1363), 369 (1773), 300 (2987), 244 (3211). ^{1}H NMR (δ ppm in DMSO-d_6): 8.98 (s, 2H, imine), 8.12 (s, 2H, protons of central aromatic ring), 7.66 (s, 2H, 2-imino-4-methylphenolic protons), 7.58 (s, 2H, pyrazolic protons), 6.99 (dd, J = 8.0, J = 1.5 Hz, 2H, 2-imino-4-methylphenolic protons), 6.73 (d, J = 8.0 Hz, 2H, 2-imino-4-methylphenolicprotons), 6.22 (bs, 1H, pyrazolic protons), 2.33 (s, 6H, CH_3), solvent peak obscures the signal arising from protons of methyl group attached to central aromatic ring.

2.5.3. [$L^{2a}Pd_2(pz)$] (3)

The complex [$L^{2a}Pd_2(pz)$] was prepared in a similar method to that of complex [$L^{1a}Pd_2(pz)$] (**1**) except that **2a** was used in the preparation instead of **1a**. Yield: 80%. *Anal.* Calc. for $C_{27}H_{24}N_4O_2Pd_2S$: C, 47.59; H, 3.55; N, 8.22; S, 4.71. Found: C, 47.47; H, 3.43; N, 8.00; S, 4.8%. IR (KBr, cm^{-1}): 3053 ν(C–H_{ar}), 2956 ν(C–H_{al}), 1669–1606 br ν(C=N_{pz}) and ν(C=N (L^{2a})), 1463 ν(C=C), 541 ν(Pd–N). UV–Vis (DMF), [λ_{max}, nm (ε, L mol^{-1} cm^{-1})]: 514 (1794), 364 (2235), 316 (3222), 241 (3251). ^{1}H NMR (δ ppm in DMSO-d_6): 9.08 (s, 2H, imine), 8.37 (s, 2H, protons of central aromatic ring), 7.85 (d, J = 8.5 Hz, 2H, *o*-iminophenolic protons) 7.56 (d, J = 1.75 Hz, 2H, pyrazolic protons),7.16 (t, J = 7.5 Hz, 2H, *o*-iminophenolic protons), 6.82 (d, J = 8.0 Hz, 2H, *o*-iminophenolic protons), 6.58 (t, J = 7.5 Hz, 2H, *o*-iminophenolic protons), 6.22 (t, J = 2.0 Hz, 1H, pyrazolic protons), 1.38 (s, 9H, *tert*-butyl).

2.5.4. [$L^{2b}Pd_2(pz)$] (**4**)

The complex [$L^{2b}Pd_2(pz)$] was prepared in a similar method to that of complex [$L^{1a}Pd_2(pz)$] (**1**) except that **2b** was used in the preparation instead of **1a**. Yield: 75%. *Anal.* Calc. for $C_{29}H_{23}N_4O_2Pd_2S$:C, 49.45; H, 3.29; N, 7.95; S, 4.55. Found: C, 49.32; H, 3.20; N, 8.09; S, 4.248%.IR (KBr, cm^{-1}): 3014 ν(C–H_{ar}), 2958 and 2920 ν(C–H_{al}), 1663–1598br ν(C=N_{pz}) and ν(C=N (L^{2b})), 1481 ν(C=C), 547 ν(Pd–N). UV–Vis (DMF), [λ_{max}, nm (ε, L mol^{-1} cm^{-1})]: 515 (1802), 365 (2611), 312 (3290), 240 (3937). ^{1}H NMR (δ ppm in DMSO-d_6): 9.04 (s, 2H, imine), 8.37 (s, 2H, protons of central aromatic ring), 7.66 (s, 2H, 2-imino-4-methylphenolic protons) 7.56 (d, J = 2.0 Hz, 2H, pyrazolic protons), 6.99 (dd, J = 8.5, J = 1.2 Hz, 2H, 2-imino-4-methylphenolic protons), 6.72 (d, J = 8.5 Hz, 2H, 2-imino-4-methylphenolic protons), 6.22 (t, J = 2.0 Hz, 1H, pyrazolic protons), 2.25 (s, 6H, CH_3), 1.38 (s, 9H, *tert*-butyl).

2.6. General procedure for the Heck cross-coupling reaction

In a round-bottom flask equipped with a magnetic stir bar, aryl halide (1.5 mmol), olefine (1 mmol), potassium carbonate (1 mmol), catalysts **1**–**4** (0.02 mmol) and DMF (2 mL) were added and heated at 100 °C. The mixture was vigorously stirred under these reaction conditions and completion of the reaction was monitored by TLC (Ethyl acetate: *n*-hexane, 25:75).

In each case, after completion of the reaction, the reaction mixture was cooled to room temperature. Then, Ethyl acetate (5 mL) and water (10 mL) were added. The aqueous layer was further extracted by ethyl acetate (2 * 5 mL). The combined organic layers were washed with saturated brine for two times, dried over $MgSO_4$, filtered, and concentrated to give the desired product.

All of compounds have been characterized by comparing their melting point, IR and ^{1}H NMR spectra with the values found in the literatures [47–51].

3. Results and discussion

3.1. Syntheses and spectroscopic characterizations

The Schiff base condensation reaction of 2 equiv. of *o*-aminophenol or 2-amino-4-methylphenol with 1 equiv. of the 2-(*N,N*-dimethylthiocarbamato)-isophthalaldehyde of 5-^{t}Bu or 5-Me lead to the formation of compartmental S-protected ligand precursors **1a**–**2b** having two available adjacent, similar coordination compartments (Scheme 1). The binuclear palladium(II) complexes **1**–**4** were synthesized by reacting the ligand precursors **1a**–**2b** with $PdCl_2$ in the presence of pyrazole at room temperature in DMSO and acetonitrile mixed solvent. The free thiophenolate ligands being liberated, via a Pd^{II}-promoted S-deprotection reaction of corresponding ligand precursors, during the formation of the complexes. These ligand precursors and binuclear palladium (II) complexes were characterized by elemental analysis, IR, ^{1}H NMR and UV–Vis spectroscopies. Infrared spectra of the ligand precursors show a band around 3366–3420 cm^{-1}, which can be ascribed to the stretching of phenolic OH group. This band has disappeared in the spectra of all the complexes, indicating the deprotonation of phenolic OH followed by coordination to the metal ion. A broad band around 1470–1600 cm^{-1} in spectra of complexes may be attributed to the stretching of C=N functional groups of Schiff-base ligands and pyrazolyl group. In ^{1}H NMR spectra of ligands, the azomethine proton (–CH=N) signal was observed at 9.22–9.27 ppm. This signal was shifted up field in the spectra of the binuclear complexes (9.00 ppm), suggesting shielding of the azomethine group in the complexes due to π-back bonding from Pd(II) [52]. The UV–Vis absorption spectra of the ligand precursors and their binuclear Pd(II) complexes were recorded in methanol and DMF solution, respectively. The precursor ligands show intense absorption bands ($\varepsilon = 10^4$–10^3 L^{-1} mol^{-1} cm^{-1}) with λ_{max} in the ranges 220–300 and 358–364 nm characteristic of, respectively, the $\pi \rightarrow \pi^*$ and $n \rightarrow \pi^*$ transitions [53–55]. The spectra of the complexes show intense absorption bands in the range 230–370 nm ($\varepsilon = 10^4$–10^3 L^{-1} mol^{-1} cm^{-1}), which are attributed to intraligand transitions. In addition, the complexes exhibit a non-ligand band around 515 nm ($\varepsilon > 10^3$ L^{-1} mol^{-1} cm^{-1}) which are attributed to the MLCT transition [56–59]. For square planar Pd(II) complexes, three spin-allowed d–d transitions $^1A_{1g} \rightarrow {}^1A_{2g}$, $^1A_{1g} \rightarrow {}^1B_{1g}$ and $^1A_{1g} \rightarrow {}^1E_g$ are expected in the visible region. In the present binulear complexes these transitions were obscured by either charge transfer or ligand bands [60,61].

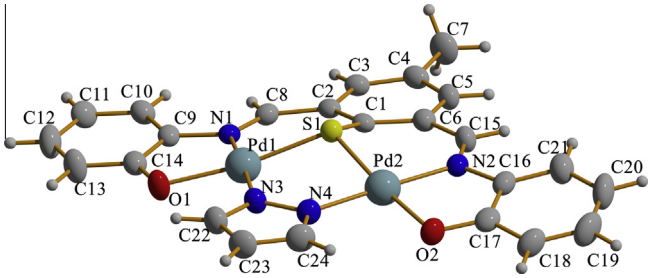

Fig. 1. Molecular structure of [$L^{1a}Pd_2(pz)$] (1), showing the atom-labeling system and 50% thermal ellipsoids.

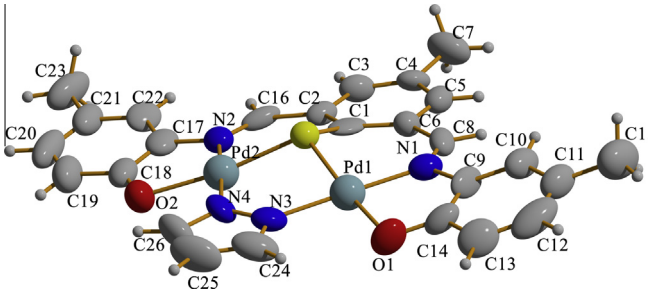

Fig. 3. Molecular structure of [$L^{1b}Pd_2(pz)$] (2), showing the atom-labeling system and 50% thermal ellipsoids.

3.2. Description of the structures

3.2.1. Crystal structure of [$L^{1a}Pd_2(pz)$] (**1**)

Fig. 1 displays the structure of the binuclear Pd^{II} molecular complex [$L^{1a}Pd_2(pz)$] (**1**), together with the atom labeling scheme. The dinuclear core consist of two palladium ions (Pd···Pd distance of 3.58(5) Å) bridged on one side by an endogenous μ-thiophenolate bridge and on the other side by an exogenous bridging pyrazolate anion. Each palladium ion is coordinated by one μ-thiophenolate S-atom, one imine N-atom, and one phenoxo O-atom of the end-off compartmental ligand system and one N-atom of the bridging pyrazolate moiety in a distorted square planar manner. The maximum deviations from the least-squares planes defined by the atoms Pd(1), N(1), N(3), S(1), O(1) and Pd(2), N(2), N(4), S(1), O (2) are 0.0157 and 0.0009 Å, respectively. The Pd–O, Pd–N and Pd–S bonds are within the normal ranges and are comparable to those observed in similar bridged palladium(II) dimers [62,63].

As shown in Fig. 2, adjacent binuclear molecules are cross-linked via π–π stacking interactions involving metal chelate–central phenyl rings and central phenyl – terminal phenyl rings (Table S1 of ESI†) to constitute an infinite 1D chain along the *a*-axis.

3.2.2. Crystal structure of [$L^{1b}Pd_2(pz)$] (**2**)

As shown in Fig. 3, the overall structure of complex [$L^{1b}Pd_2(pz)$] (**2**) is analogous to that of [$L^{1a}Pd_2(pz)$] (**1**). The intramolecular Pd (1)···Pd(2) separation is 3.57(16) Å in this molecule. The maximum deviations from the least-squares planes defined by the atoms Pd(1), N(1), N(3), S(1), O(1) and Pd(2), N(2), N(4), S(1), O(2) are 0.0067and 0.0073 Å, respectively.

As shown in Fig. 4, adjacent binuclear molecules along the *a*-axis are linked by a number of π–π stacking interactions (involving metal chelate–central phenyl rings, central phenyl – terminal phenyl rings and terminal phenyl– terminal phenyl rings) (Table S1 of ESI†) and weak C–H···N interactions between C(23)–H(23B)···N(3)^{i} (symmetry code (i): 3 − *X*, −*Y*, −*Z*) with bond lengths H(23B)···N(3) 2.67(10) Å, C(23)···N(3) 3.62(18) Å and angle C(23)–H(23B)···N(3) 173.57(10)°, forming a 1D chain.

3.2.3. Crystal structure of [$L^{2a}Pd_2(pz)$] (**3**)

The overall structure of complex [$L^{2a}Pd_2(pz)$] (**3**) is similar to that of [$L^{1a}Pd_2(pz)$] (**1**) and [$L^{1b}Pd_2(pz)$] (**2**), as shown in Fig. 5. The intramolecular Pd(1)···Pd(2) separation is 3.57(8) Å in this molecule. The maximum deviations from the least-squares planes defined by the atoms Pd(1), N(1), N(3), S(1), O(1) and Pd(2), N(2), N (4), S(1), O(2) are 0.0142 and 0.0127 Å, respectively. Within the crystal structure, the methyl groups of the *tert*-butyl residue were found to be disordered over two positions with occupancies of between 26% and 74%. Temperature factors of these methyl groups are considerably large owing to the thermal motion and rotation. In packing structure, π-stacking manner in **3** is much different from that of complexes **1** and **2**. As shown in Fig. 6, the orientation of the binuclear molecules in the crystal lattice is in such a manner that π···π stacking interactions involving metal chelate, pyrazolate and terminal phenyl rings reinforce the packing (Table S1 of ESI†).

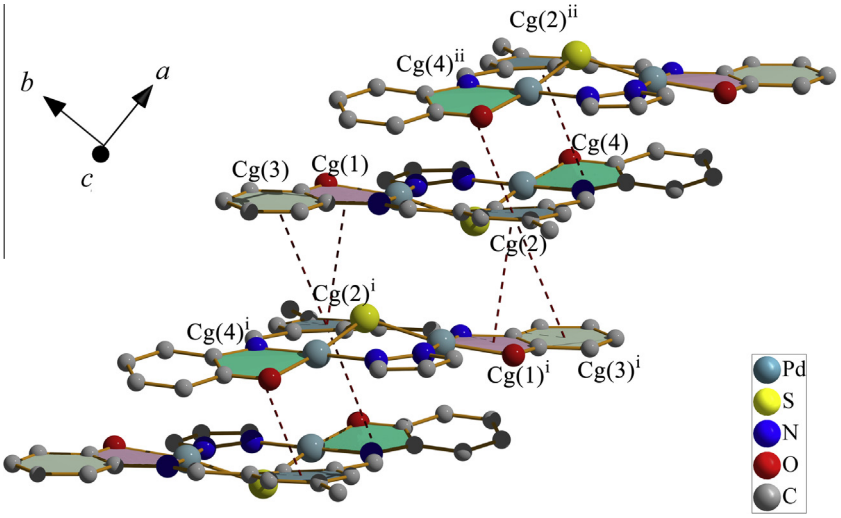

Fig. 2. Perspective view of the formation of a 1Dchain in [$L^{1a}Pd_2(pz)$] (1) formed through π–π stacking interactions along the *a*-axis direction. Hydrogen atoms are omitted for clarity.

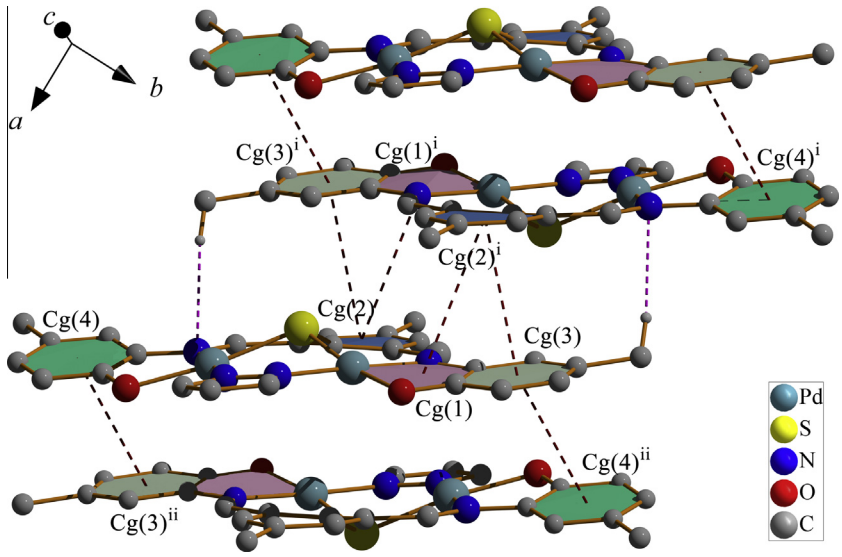

Fig. 4. Perspective view of the formation of a 1D chain in [$L^{1b}Pd_2(pz)$] (2) formed through non-classical hydrogen bonds and π–π stacking interactions along the *a*-axis direction. Hydrogen atoms, except those involved in hydrogen-bonding interactions, are omitted for clarity.

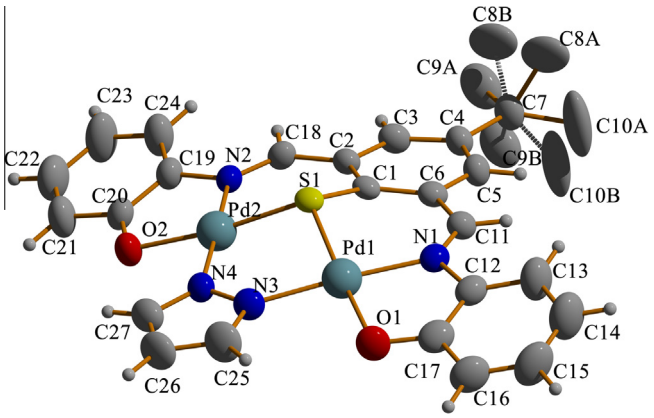

Fig. 5. Molecular structure of [$L^{2a}Pd_2(pz)$] (3), showing the atom-labeling system and 50% thermal ellipsoids.

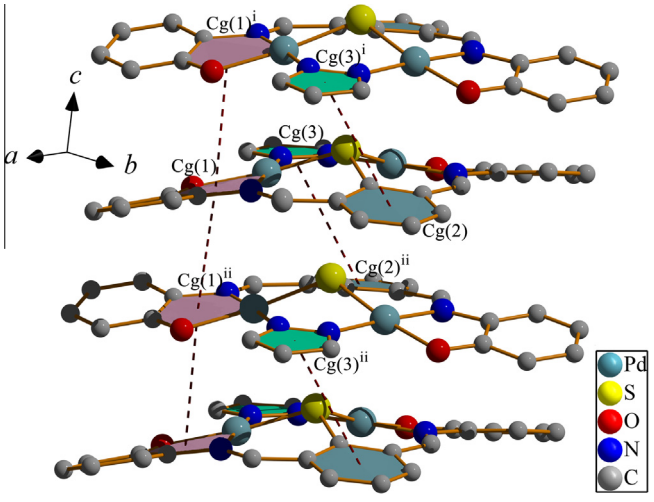

Fig. 6. Perspective view of the formation of a 1D chain in [$L^{2a}Pd_2(pz)$](**3**) formed through π–π stacking interactions along the *c*-axis direction. Hydrogen atoms and *tert*-butyl groups are omitted for clarity.

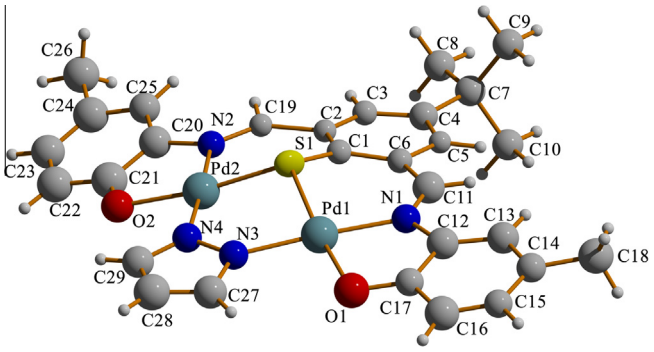

Fig. 7. Molecular structure of [$L^{2b}Pd_2(pz)$] (**4**), showing the atom-labeling system.

These interactions propagate, leading to the formation of a 1D chain along the *c*-axis.

*3.2.4. Crystal structure of [$L^{2b}Pd_2(pz)$] (**4**)*

Although the analytical and spectroscopic data show the presence of a dinuclear Pd_2-core as the smallest unit in complex **4**, an X-ray analysis was undertaken to remove any doubts regarding its structure. Unfortunately, crystals of [$L^{2b}Pd_2(pz)$] (**4**) [$C_{29}H_{23}N_4O_2Pd_2S$] were twinned and diffracted very weak. The unit cell contains two independent dinuclear Pd. In spite of its high *R* factor and large standard deviations, the crystal structure analysis of **4** confirmed its dinuclear structure (Fig. 7). Because of its unacceptable quality, we are refraining from publishing the crystal data in detail. The structure of **4** is similar to that of the other complexes **1**–**3**. The intramolecular Pd(1)···Pd(2) separation is 3.57(25) Å in this molecule. The maximum deviations from the least-squares planes defined by the atoms Pd(1A), N(1A), N(3A), S(1A), O(1A) and Pd(2A), N(2A), N(4A), S(1A), O(2A) and Pd(1B), N(1B), N(3B), S(1B), O(1B) and Pd(2B), N(2B), N(4B), S(1B), O(2B) are 0.0082 and 0.0106 Å, 0.0050 and 0.0086 Å, respectively.

The crystal packing structure of complex [$L^{2b}Pd_2(pz)$] (**4**) is similar to that of complex [$L^{2a}Pd_2(pz)$] (**3**), stabilized via "metal chelate–metal chelate ring" and "terminal phenyl–pyrazolate ring" π–π stacking interactions between adjacent binuclear molecules to form a 1D chain along the *a*-axis (Fig. 8, Table S1 of ESI†).

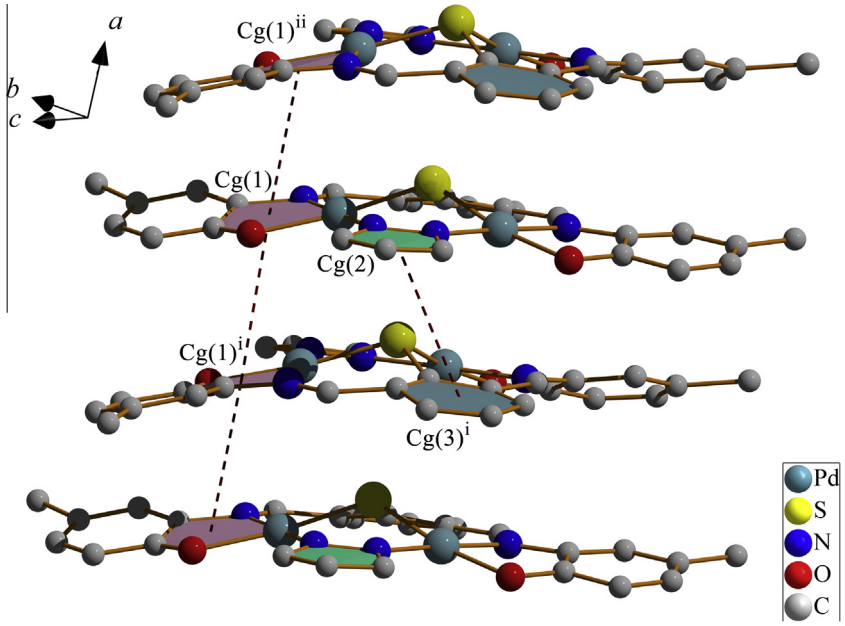

Fig. 8. Perspective view of the formation of a 1D chain in [$L^{2b}Pd_2(pz)$](**4**) formed through π–π stacking interactions along the *a*-axis direction. Hydrogen atoms and *tert*-butyl groups are omitted for clarity.

Table 3
Optimization of Heck coupling reaction conditions between methyl acrylate and bromobenzene.[a]

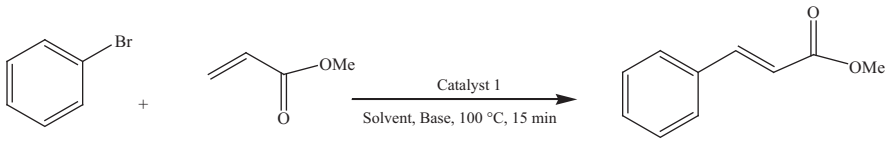

Entry	Solvent	Base	Catalyst (mol%)	Conversions (%)[b]
1	DMF	K_2CO_3	5	78
2	Toluene	K_2CO_3	5	54
3	THF	K_2CO_3	5	48
4	H_2O	K_2CO_3	5	16
5	EtOH	K_2CO_3	5	22
6	DMF	NaOAc	5	56
7	DMF	Et_3N	5	41
8	DMF	K_2CO_3	None	ND[c]
9	DMF	K_2CO_3	0.5	57
10	DMF	K_2CO_3	2	77
11	DMF	K_2CO_3	10	80

[a] Reaction conditions: bromobenzene (1.5 mmol), methylacrylate (1 mmol), Base (1 mmol), catalyst, solvent (2 mL), 100 °C and 15 min.
[b] Using gas chromatography.
[c] Not detected.

3.3. Catalytic activity

After confirming the exact structure and characteristics of all the complexes, we decided to examine their catalytic activities in organic reactions. To this end, we chose the Heck coupling reaction, the most important reaction that changed the chemistry world in recent years thoroughly, especially in the field of catalysis. The results demonstrated excellent catalytic activity and efficiency of these catalysts. So, all four synthesized catalytic systems were employed in these reactions to compare their activity in the Heck coupling reaction.

Initially, reaction conditions were optimized and Heck coupling between methyl acrylate and bromobenzene was selected as the model reaction (Table 3). To this end, various types of solvents and bases were employed in the model reaction in the presence of 2 mol% of complex [$L_1aPd_2(pz)$] (**1**) as catalyst at 100 °C. In addition, concentration of catalyst was also optimized and finally DMF was selected as the best solvent and K_2CO_3 as the optimum base. Also, the best results were obtained in the presence of 2 mol% of catalystat 100 °C (Table 3, entry 10).

These conditions were used for conducting all the C–C coupling reactions. Furthermore, having a reasonable comparison between the catalytic activities of four palladium-based complexes, these conditions were also used to conduct the reactions using other three catalytic systems. Results are listed in Table 4. As can be seen, various types of aryl halides including both electron-donating and electron-withdrawing groups were used in the Heck reaction with methyl acrylate and butyl acrylate as alkene, the second coupling partner. Furthermore, reactions were performed using both aryl iodides and aryl bromides and in both cases, very good to excellent yields were obtained in the range of 30–140 min. When chlorobenzene was used, reaction failed to be completed and its yield was

Table 4
Heck coupling reaction of various aryl halides and alkenes under optimized conditions.[a]

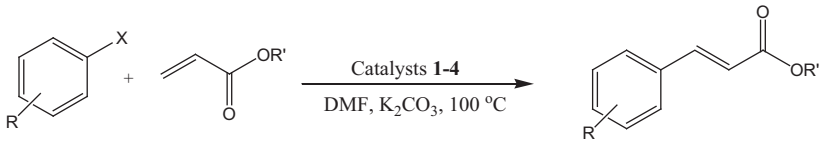

Entry	ArX	Alkene	Product	Time (min)	Conversions (%)[b]			
					1	**2**	**3**	**4**
1	Iodobenzene	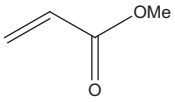	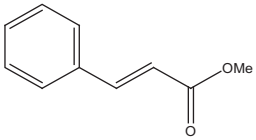	30	>99	>99	>99	>99
2	Bromobenzene		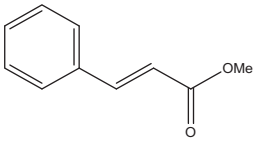	30	95	95	96	96
3	Chlorobenzene		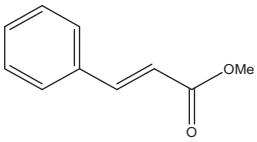	70	20	18	21	24
4	1-Bromonaphthalene		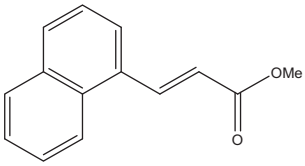	100	>99	>99	>99	>99
5	4-Bromotoluene		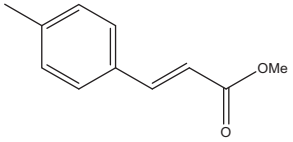	35	>99	>99	>99	>99
6	4-Bromoacetophenone		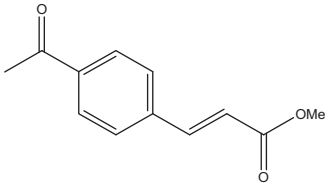	60	>99	>99	>99	>99
7	4-Bromobenzaldehyde		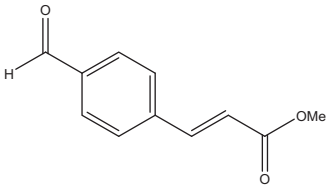	60	>99	>99	>99	>99
8	4-Bromoanisole		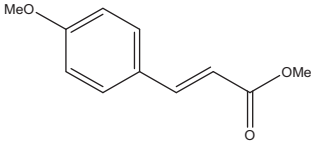	60	ND[c]	ND	ND	ND
9	Iodobenzene	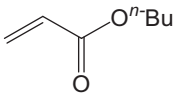	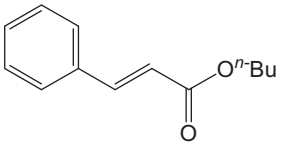	60	>99	>99	>99	>99
10	Bromobenzene		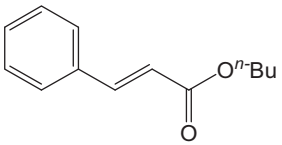	60	>99	>99	>99	>99

Table 4 (*continued*)

Entry	ArX	Alkene	Product	Time (min)	Conversions (%)[b]			
					1	**2**	**3**	**4**
11	1-Bromonaphthalene		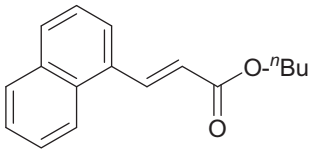	140	>99	>99	>99	>99

[a] Reaction Conditions: aryl halide (1.5 mmol), methyl/*n*-butyl acrylate (1 mmol), K_2CO_3(1 mmol), DMF (2 mL), Catalyst (2 mol%) and 100 °C.
[b] Using gas chromatography.
[c] Not detected.

Table 5
Comparison of Heck coupling of bromobenzene with *n*-butylacrylate using [LPd_2(pz)] and other catalytic systems.

Entry	Catalyst	Conditions	Conversion [%]	Time (h)	Ref.
1	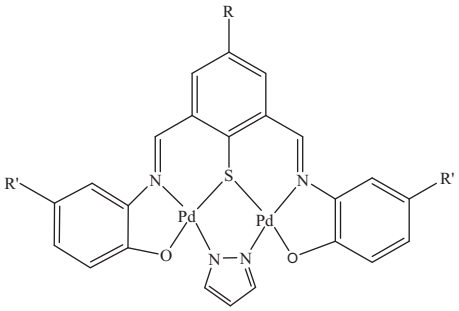	0.02 mmol catalyst, 1.5 mmol Bromobenzene, 1 mmol *n*-butylacrylate, 1 mmol K_2CO_3, 2 mL DMF, 100 °C	>99	1	Present work
2	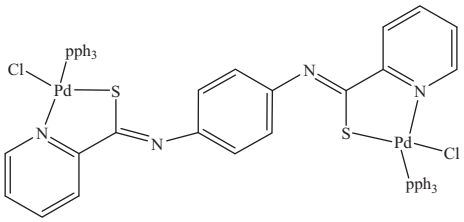	0.01 mmol catalyst, 1 mmol Bromobenzene, 2 mmol *n*-butylacrylate, 1.2 mmol K_2CO_3, 2 mL DMF, 150 °C	96	20	[64]
3	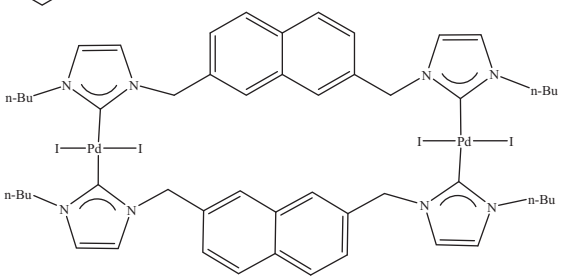	0.01 mmol catalyst, 1 mmol Bromobenzene, 1.4 mmol *n*-butylacrylate, 1.1 mmol *i*-Pr_2NEt, 0.1 mmol HCOONa, 2.5 ml DMF, 120 °C	5	24	[65]
4	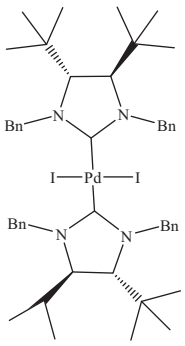	0.02 mmol catalyst, 1 mmol Bromobenzene, 1.5 mmol *n*-butylacrylate, 1.5 mmol HCOONa, 1 mL DMF, 120 °C	2	16	[66]
5	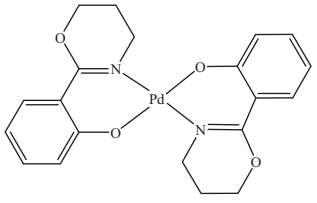	0.01 mmol catalyst, 1 mmol Bromobenzene, 1.1 mmol *n*-butylacrylate, 1.1 mmol NEt_3, 1 mL DMA, 120 °C	83	8	[67]

not significant (Table 4, entry 3). From the stereochemical view point, both *cis* and *trans* isomers of the coupled products can be obtained in these reactions, but using all these proposed catalysts, only *trans* isomers were obtained stereoselectively. This fact can be found easily from the coupling constants of olefinic protons in ^{1}H NMR spectra. So, it is noteworthy that the reactions are carried out in a stereospecific manner and in each case no *cis* isomer of the product was detected. Results of all four complexes were comparable; in each case, reactions were performed completely.

FT IR spectra of the complex **1** were recorded before and after the reaction (Fig. S12). As can be seen clearly, the characteristic peaks verifying the structure of the complex were remained unchanged; so, considering the similarity between catalyst's structures, it could be concluded that none of the catalysts has changed during the course of the reaction.

We used the reaction of bromobenzene with *n*-butyl acrylate to compare the efficacy of the [$LPd_2(pz)$] with other reported catalysis systems (Table 5). Several goals have to be achieved for the utilization of aryl bromides in Heck reaction, such as the use of stable and inexpensive starting materials and ligands and achievement of high conversions and yields. However, the high reaction temperature and long reaction times in some reported systems are not beneficial to the industrial and synthetic applications (entries 2–5). In addition, some catalyst systems create practical problems because of high ligand sensitivity toward air and moisture and multistep synthesis procedures (entries 2–4). Table 5 illustrates that the [$LPd_2(pz)$] gives higher yield at the much lower reaction time and temperature in comparison with other systems.

4. Conclusion

We have synthesized and characterized three new binucleating S-protected ligand precursors **1b**, **2a** and **2b**. Four new binuclear palladium(II) complexes with the general formula [$LPd_2(pz)$] have been synthesized by reacting the binucleating S-protected ligand precursors **1a**–**2b** with palladium(II) chloride in the presence of pyrazole. Analytical, spectral (IR, UV–Vis, ^{1}H NMR) and X-ray diffraction studies revealed that the two palladium ions are doubly bridged by a common exogenous bridging pyrazolate group and an endogenous bridging thiophenolate-sulfur atom with a Pd···Pd distance of 3.57 Å. Furthermore, the catalytic behavior of these complexes was investigated in the Heck reaction. All the complexes could catalyze the C–C coupling reaction between methyl- and butyl acrylate with different types of aryl halides including aryl iodides and bromides. In addition, the presence of electron-donating or electron-withdrawing groups on the phenyl ring of aryl halides could not limit the scope of the reactions; reaction times were very short and reactions were performed with full conversions and excellent yields.

Acknowledgment

The authors are grateful to the Research Council of Sharif University of Technology, Iran for their financial support.

Appendix A. Supplementary material

CCDC 1061222 (complex **1**), 1061223 (complex **2**), 1061224 (complex **3**) contains the supplementary crystallographic data for this paper. These data can be obtained free of charge from The Cambridge Crystallographic Data Centre via www.ccdc.cam.ac.uk/data_request/cif. Supplementary data associated with this article can be found, in the online version, at http://dx.doi.org/10.1016/j.ica.2015.10.035.

References

[1] K.C. Nicolaou, P.G. Bulger, D. Sarlah, Angew. Chem., Int. Ed. 44 (2005) 4442.
[2] X. Chen, K.M. Engle, D.-H. Wang, J.-Q. Yu, Angew. Chem., Int. Ed. Engl. 48 (2009) 5094.
[3] C. Barnard, Platin. Met. Rev. 52 (2008) 38.
[4] L. Yin, J. Liebscher, Chem. Rev. 107 (2007) 133.
[5] S.B. Park, H. Alper, Org. Lett. 5 (2003) 3209.
[6] F. Diederich, P.J. Stang, Metal-Catalyzed Cross-Coupling Reactions, John Wiley & Sons, 2008.
[7] I.P. Beletskaya, A.V. Cheprakov, Chem. Rev. 100 (2000) 3009.
[8] G.T. Crisp, Chem. Soc. Rev. 27 (1998) 427.
[9] S.O. Ojwach, I.A. Guzei, J. Darkwa, S.F. Mapolie, Polyhedron 26 (2007) 851.
[10] P. Pelagatti, M. Carcelli, M. Costa, S. Ianelli, C. Pelizzi, D. Rogolino, J. Mol. Catal. A: Chem. 226 (2005) 107.
[11] D. Kovala-Demertzi, P.N. Yadav, M.A. Demertzis, J.P. Jasiski, F.J. Andreadaki, I.D. Kostas, Tetrahedron Lett. 45 (2004) 2923.
[12] W.A. Herrmann, C. Reisinger, M. Spiegler, J. Organomet. Chem. 557 (1998) 93.
[13] W. Chen, C. Xi, Y. Wu, J. Organomet. Chem. 692 (2007) 4381.
[14] W.M. Motswainyana, M.O. Onani, Inorg. Chem. Commun. 24 (2012) 221.
[15] T. Zhao, Q. Xing, K. Song, Q. Ban, T. Liang, Q. Liu, W.-H. Sun, RSC Adv. 5 (2015) 14228.
[16] A.L. Balch, B.J. Davis, E.Y. Fung, M.M. Olmstead, Inorg. Chim. Acta 212 (1993) 149.
[17] C.J. McKenzie, R. Robson, J. Chem. Soc., Chem. Commun. (1988) 112.
[18] T. Hu, Y.-G. Li, Y.-S. Li, N.-H. Hu, J. Mol. Catal. A: Chem. 253 (2006) 155.
[19] C. Cao, Y. Zhuang, J. Zhao, Y. Peng, X. Li, Z. Shi, G. Pang, Y. Shi, Inorg. Chim. Acta 363 (2010) 3914.
[20] B. Banik, A. Tairai, N. Shahnaz, P. Das, Tetrahedron Lett. 53 (2012) 5627.
[21] D. Yuan, H.V. Huynh, Organometallics 29 (2010) 6020.
[22] N. Tsukada, T. Mitsuboshi, H. Setoguchi, Y. Inoue, J. Am. Chem. Soc. 125 (2003) 12102.
[23] V.K. Jain, L. Jain, Coord. Chem. Rev. 249 (2005) 3075.
[24] J. Chu, X. Xie, S. Yang, S. Zhan, Inorg. Chim. Acta 410 (2014) 191.
[25] A.L. Gavrilova, B. Bosnich, Chem. Rev. 104 (2004) 349.
[26] A. Lennartson, V. Mckee, J. Nelson, M. Arthurs, C.J. McKenzie, Supramol. Chem. 24 (2012) 604.
[27] B.F. Hoskins, R. Robson, G.A. Williams, J.C. Wilson, A. Williams, Inorg. Chem. 30 (1991) 4160.
[28] V. Lozan, J. Hunger, B. Kersting, Inorg. Chim. Acta 360 (2007) 3189.
[29] A.L. Gavrilova, B. Bosnich, Chem. Rev. 104 (2004) 349.
[30] B. Krebs, G. Henkel, Angew. Chem., Int. Ed. Engl. 30 (1991) 769.
[31] W. Mazurek, A.M. Bond, K.S. Murray, M.J. O'Connor, A.G. Wedd, Inorg. Chem. 24 (1985) 2484.
[32] S. Gruschinski, M. Handke, B. Kersting, Zeitschrift Für Anorg. Und Allg. Chem. 638 (2012) 1274.
[33] S. Brooker, Coord. Chem. Rev. 222 (2001) 33.
[34] D. Herebian, E. Bothe, E. Bill, T. Weyhermuller, K. Wieghardt, J. Am. Chem. Soc. 123 (2001) 10012.
[35] L.M. Peschel, C. Holzer, L. Mihajlović-Lalić, F. Belaj, N.C. Mösch-Zanetti, Eur. J. Inorg. Chem. (2015) 1569.
[36] A. Beganskiene, L.R. Pignotti, V. Baltramiejunaite, R.L. Luck, E. Urnezius, Inorg. Chim. Acta 361 (2008) 1349.
[37] A. Christensen, C. Mayer, F. Jensen, A.D. Bond, C.J. McKenzie, Dalton Trans. (2006) 108.
[38] M. Louey, P.D. Nichols, R. Robson, Inorg. Chim. Acta 47 (1980) 87.
[39] P. Iliopoulos, K.S. Murray, R. Robson, J. Wilson, G.A. Williams, J. Chem. Soc., Dalton Trans. (1987) 1585.
[40] J.G. Hughes, R. Robson, Inorg. Chim. Acta 36 (1979) 237.
[41] N. Khadir, D.M. Boghaei, A. Assoud, O.R. Nascimento, A. Nicotina, L. Ghivelder, R. Calvo, Dalton Trans. 44 (2015) 2431.
[42] S. Brooker, P.D. Croucher, F.M. Roxburgh, J. Chem. Soc., Dalton Trans. (1996) 3031.
[43] S. Brooker, G.B. Caygill, P.D. Croucher, T.C. Davidson, D.L.J. Clive, S.R. Magnuson, S.P. Cramer, C.Y. Ralston, J. Chem. Soc., Dalton Trans. (2000) 3113.
[44] Bruker Saint Plus Data Reduction and Correction Program, V. 6.01, Bruker AXS, Madison Wisconsin, USA, Madison, Wisconsin, USA, 1998.
[45] G.M. Sheldrick, SADABS Siemens Area Detector Absorption Correction Program, v. 2.01, Bruker/Siemens, Madison, Wisconsin, USA, 1998.
[46] G.M. Sheldrick, SHELXTL. Structure Determination Software Suite, v.5.1, Bruker, Madison, Wisconsin, USA, 1998.
[47] F. Zhao, M. Arai, React. Kinet. Catal. Lett. 81 (2004) 281.
[48] F. Zhao, B.M. Bhanage, M. Shirai, M. Arai, React. Kinet. Catal. Lett. 6 (2000) 843.
[49] A. Spencer, J. Organomet. Chem. 270 (1984) 115.
[50] C.B. Z.Jr, R.F. Heck, J. Org. Chem. 43 (1978) 2949–2952.
[51] P. Wang, H. Liu, M. Liu, R. Li, J. Ma, New J. Chem. 38 (2014) 1138.
[52] D. Kovala-Demertzi, A. Alexandratos, A. Papageorgiou, P.N. Yadav, P. Dalezis, M.A. Demertzis, Polyhedron 27 (2008) 2731.
[53] S. Mandal, B. Naskar, R. Modak, Y. Sikdar, S. Chatterjee, S. Biswas, T.K. Mondal, D. Modak, S. Goswami, J. Mol. Struct. 1088 (2015) 38.
[54] L.-L. Fan, F.-S. Guo, L. Yun, Z.-J. Lin, R. Herchel, J.-D. Leng, Y.-C. Ou, M.-L. Tong, Dalton Trans. 39 (2010) 1771.
[55] P. Pattanayak, D. Patra, P. Brandão, D. Mal, V. Felix, Inorg. Chem. Commun. 53 (2015) 68.

[56] M. Yoshizawa, K. Ono, K. Kumazawa, T. Kato, M. Fujita, J. Am. Chem. Soc. 127 (2005) 10800.
[57] S.-W. Lai, T.-C. Cheung, M.C.W. Chan, K.-K. Cheung, S.-M. Peng, C.-M. Che, Inorg. Chem. 39 (2000) 255.
[58] S.Ø. Scottwell, K.J. Shaffer, C.J. McAdam, J.D. Crowley, RSC Adv. 4 (2014) 35726.
[59] A.J. Hallett, C.J. Adams, K.M. Anderson, R.A. Baber, N.G. Connelly, C.J. Prime, Dalton Trans. 39 (2010) 5899.
[60] P.A. Ajibade, O.G. Idemudia, Bioinorg. Chem. Appl. 2013 (2013) 1.
[61] P. Kalyani, M. Adharvanachary, P.M.M.S. Kinthada, Int. J. Pharm. Biomed. Sci. 3 (2012) 75.
[62] B.F. Hoskins, Aust. J. Chem. 37 (1984) 1395.
[63] B.F. Hoskins, Aust. J. Chem. 37 (1984) 725.
[64] M.U. Raja, R. Ramesh, Y. Liu, Tetrahedron Lett. 52 (2011) 5427.
[65] S. Saito, M. Saika, R. Yamasaki, I. Azumaya, H. Masu, Organometallics 30 (2011) 1366.
[66] J. Pytkowicz, S. Roland, P. Mangeney, G. Meyer, A. Jutand, J. Organomet. Chem. 678 (2003) 166.
[67] M. Bagherzadeh, M. Amini, A. Ellern, L. Keith Woo, Inorg. Chim. Acta 383 (2012) 46–51.